Accepted Manuscript

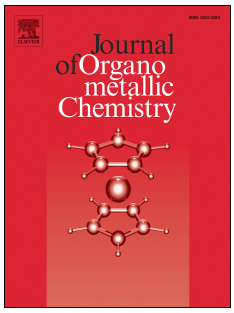

Radiosynthesis and evaluation of novel $^{99m}Tc(CO)_3$-labelled thymidine dithiocarbamate derivatives for tumor imaging with SPECT

Xiaojiang Duan, Qing Ruan, Qianqian Gan, Xiaoqing Song, Si'an Fang, Xuran Zhang, Junbo Zhang

PII: S0022-328X(18)30334-6

DOI: 10.1016/j.jorganchem.2018.05.009

Reference: JOM 20443

To appear in: *Journal of Organometallic Chemistry*

Received Date: 19 February 2018

Revised Date: 8 May 2018

Accepted Date: 9 May 2018

Please cite this article as: X. Duan, Q. Ruan, Q. Gan, X. Song, Si'. Fang, X. Zhang, J. Zhang, Radiosynthesis and evaluation of novel $^{99m}Tc(CO)_3$-labelled thymidine dithiocarbamate derivatives for tumor imaging with SPECT, *Journal of Organometallic Chemistry* (2018), doi: 10.1016/j.jorganchem.2018.05.009.

Radiosynthesis and evaluation of novel $^{99m}Tc(CO)_3$-labelled thymidine dithiocarbamate derivatives for tumor imaging with SPECT

Xiaojiang Duan [a], Qing Ruan [a], Qianqian Gan [a], Xiaoqing Song [a], Si'an Fang [a], Xuran Zhang [a, b], and Junbo Zhang*

[a] Key Laboratory of Radiopharmaceuticals (Beijing Normal University), Ministry of Education, College of Chemistry, Beijing Normal University, Beijing 100875, China.
[b] Department of Isotopes, China Institute of Atomic Energy, P. O. Box 2108, Beijing 102413, China
*Corresponding Author:
For Junbo Zhang: phone +86-10-62208126, E-mail zhjunbo@bnu.edu.cn.

Abstract:

A series of novel thymidine dithiocarbamate derivatives (DTC-TdR) were successfully synthesized and then radiolabelled using $[^{99m}Tc(CO)_3]^+$ core with high yields. The chemical characterizations of $^{99m}Tc(CO)_3$-labelled dithiocarbamate derivatives have been carried out by preparing their corresponding rhenium complexes. The radiotracers were stable *in vitro*, and the partition coefficient results indicated that they were lipophilic. The cell uptake studies showed the uptakes of these $^{99m}Tc(CO)_3$-labelled thymidine derivatives were mediated by nucleoside transporters. Biodistribution of the complexes in mice bearing tumor showed that they had high tumor uptake and good tumor/muscle ratio. A clear SPECT imaging of the tumor location was obtained in mice bearing S180 tumor with one of radiotracers, suggesting they would be potential tumor imaging agents.

1. Introduction

As the most established radiotracer for positron emission tomography (PET), the uptake of ^{18}F-FDG (2-[^{18}F]fluoro-2-deoxy-D-glucose) is strongly related with glucose metabolism [1]. Due to the presence of the Warburg effect, the uptake of ^{18}F-FDG in tumor is usually significantly increased [2], making it the gold standard radiotracer for tumor detection and clinical staging. While ^{18}F-FDG also accumulates in brain, inflammatory lesions and other metabolically active organs [3]. Sustained proliferation is one of the hallmarks of cancer[4], and DNA synthesis is the most

reliable marker for cell proliferation. For years, nucleoside and nucleoside analogs, including some nucleoside complexes, have played an important role in the diagnosis and treatment of cancer and viral diseases [5-9]. Thymine is the only base that incorporates DNA rather than RNA, and the metabolic process of thymidine is the most specific way to measure cell proliferation. To overcome the shortcomings of ^{18}F-FDG, ^{18}F-FLT (3'-deoxy-3'-[^{18}F]fluorothymidine), has been proposed as a radiotracer for cell proliferation imaging [10]. As an analog of thymidine deoxyribose (TdR), ^{18}F-FLT is taken up by cell via the same mechanisms as nucleoside thymidine, and then phosphorylated by thymidine kinase 1 (TK1), resulting trapped in the cell [11]. ^{18}F-FLT is an effective tracer of tumor proliferation, and is a specific, prognostic predictor in the clinical treatment of cancer [12]. Compared to the positron nuclide ^{18}F, generator produced isotope ^{99m}Tc can be obtained at a reasonable cost. In addition, ^{99m}Tc has suitable physical characteristics (E_γ = 140 keV, $T_{1/2}$ = 6.02 h), versatile chemistry due to its multi-oxidation states and the ability to produce a variety of complexes, being the major advantages of ^{99m}Tc as a radionuclide for radiopharmaceutical development. Thus, using ^{99m}Tc to label thymidine derivatives has always attracted the attention of researchers.

To date, many ^{99m}Tc labelled thymidine derivatives have been prepared [13-22]. In 2003, R. Schibi *et al.* prepared six $M(CO)_3$ (M= ^{99m}Tc, Re) labelled 5'-carboxamide derivatives of 5'-aminothymidine and the affinity of the rhenium-tricarbonyl compounds were evaluated *in vitro* with TK-1 [13]. M. Stichelberger *et al.* synthesized several $M(CO)_3$-complexes (M= ^{99m}Tc, Re), and evaluated them *in vitro*. The mixed inhibition of TK-1 was observed with K_i values ranging from 4.4 to 334 μM. Then S. Celen *et al.* synthesized ^{99m}Tc-MAMA-propyl-thymidine (3-N-[S-trityl-2-mercaptoethyl]-N-[NV-(S-trityl-2-mercaptoethyl)amidoacetyl]-amino propyl-thymidine), a derivative at position N3 of thymidine. Unfortunately, unlike the clear uptake of ^{18}F-FLT can be visualized with μPET, ^{99m}Tc-MAMA-propyl-thymidine had no uptake in the tumor sites, probably due to the bulky ^{99m}Tc-MAMA ligand [15]. D. Desbouis *et al.* also prepared a series of thymidine derivatives labelled with the $M(CO)_3$ core (M= ^{99m}Tc, Re). The complexes carried different charges: neutral, cationic and anionic. The neutral, lipophilic complexes with a log *P* value > 1 had a higher phosphorylation rate in phosphorylation assay and a higher uptake in a human neuroblastoma cell line (SKNMC) *in vitro* cell internalization experiments [18]. Similarly, H. Struthers *et al.* also found neutral or cationic compounds maintained

substrate activity towards the TK-1 [19, 20] for the N3-functionalized derivatives. In view of the fact that ^{99m}Tc-tricarbonyl complexes tend to be rather lipophilic in comparison to other ^{99m}Tc complexes, the ^{99m}Tc tricarbonyl complexes of thymidine analogs are more likely to be the imaging agent we are striving for. In the previous work of our group, a series of $^{99m}Tc(CO)_3$-labelled macrocylic triamine-derivatised thymidine analogs have been prepared and their biodistributions were systematically evaluated [23]. However, due to the fact that the ligand moiety was too bulky, the biological properties of those complexes were not satisfactory.

Dithiocarbamate (DTC) is a kind of ligand with low charge and relatively small pitch, which can be strongly complexed with metal ions. Based on our previous reported work [24-32], thymidine dithiocarbamate analog can be assumed to form stable ^{99m}Tc-tricarbonyl complex on the basis of efficient binding of the sulfur atoms. In this study, novel thymidine dithiocarbamate analogs functionalized at position N3 of thymidine were successfully synthesized, and then labelled by $M(CO)_3$ core (M= ^{99m}Tc, Re) to prepare the corresponding complexes. The partition coefficients, stability *in vitro*, *in vitro* cell internalization experiments, biodistribution and SPECT/CT imaging in mice bearing tumor were also evaluated.

2. Materials and methods

2.1. Materials and measurements

All A.R. grade chemical reagents used in synthesis were purchased from commercial sources and were used without any further purification. The ^{99}Mo/^{99m}Tc generator was obtained from Beijing Atomic High-Tech Co. The ^{1}H NMR spectra and ^{13}C NMR spectra were obtain at 400 MHz and 100MHz on a Bruker spectrometer, respectively (Bruker, Billerica, MA, USA). Mass spectrometry were performance on the LC-MS Shimadzu 2010 series (Shimadzu, Kyoto, Japan). The HRMS spectra were acquired from AB SCIEX TripleTOF^{TM} 5600 (AB Sciex, Concord, Canada). IR spectrum was obtained with an AVATAR 360 FT-IR spectrometer using KBr pellets. Radiochemical purity was determined by HPLC performed on a Waters 600 binary HPLC pump and a Waters 2489 UV absorbance dual detector (Waters, Milford, USA) with a reversed-phase C-18 column (Kromasil C18, 4.6 mm 250 mm). The murine sarcoma S180 cell line was purchased from Peking University Health Science Center (Beijing, China). HCT116 cell line was obtained from China Infrastructure of Cell Line Resource (Beijing, China).

2.2. Methods

2.2.1. Synthesizes of thymidine dithiocarbamates

Compound **1-4** were prepared by multi-step reactions from initial material thymidine. The reaction route of **1-4** were shown in Scheme 1. Compound **5** was synthesized according to the literature reported by Tronchet *et al* [33].

*2.2.1.1. General procedure for the preparation of **6-9***

Compound **6-9** was prepared according the literature reported by Cheng L *et.al* [34] and with some modifications. Namely, phthalimide (2.9 g, 20 mmol) and the appropriate dibromoalkanes (80 mmol) were added into MeCN (50 mL). After an addition of K_2CO_3 (11 g, 80 mmol), the mixture was refluxed for 24 h and followed by TLC (Thin Layer Chromatography). The solvent was evaporated under reduced pressure, and then the residuum was dissolved in ethyl acetate (200 mL) and washed by water (3×100 mL). The organic phase was dried by $MgSO_4$, and then was evaporated. The crude product was purified by column chromatography (PE/EtOAc = 10:1, R_f = 0.4) to give **6-9**.

Compound **6** (white solid, 3.6 g, yield 70.9%). ^{1}H-NMR (400 MHz, Chloroform-d) δ 7.86 – 7.80 (m, 2H), 7.74 – 7.68 (m, 2H), 3.71 (t, J = 6.7 Hz, 2H), 3.43 (t, J = 6.3 Hz, 2H). ^{13}C NMR (100 MHz, Chloroform-d) δ 167.91, 134.35, 131.97, 123.63, 39.42, 28.29. MS (*m/z*): 254.1 (calc. 254.0 $[C_{10}H_8BrNO_2]H^+$).

Compound **7** (white solid, 3.7 g, yield 69.0%). ^{1}H NMR (400 MHz, Chloroform-*d*) δ 7.90 – 7.79 (m, 2H), 7.73 (m, 2H), 3.84 (q, J = 6.7 Hz, 2H), 3.42 (q, J = 6.4 Hz, 2H), 2.26 (dq, J = 13.2, 6.5, 5.5 Hz, 2H). MS (*m/z*): 268.0 (calc. 268.0 $[C_{11}H_{10}BrNO_2]H^+$).

Compound **8** (white solid, 4.7 g, yield 83%). ^{1}H NMR (400 MHz, Chloroform-*d*) δ 7.87 – 7.78 (m, 2H), 7.75 – 7.66 (m, 2H), 3.71 (t, J = 6.7 Hz, 2H), 3.43 (t, J = 6.4 Hz, 2H), 1.95 – 1.78 (m, 4H). ^{13}C NMR (100 MHz, Chloroform-*d*) δ 167.94, 133.74, 131.77, 122.93, 36.69, 32.80, 29.66, 27.02. MS (*m/z*): 282.0 (calc. 282.0 $[C_{12}H_{12}BrNO_2]H^+$).

Compound **9** (colorless oil, 4.8 g, yield 80.4%).^{1}H NMR (400 MHz, Chloroform-d) δ 7.73 (dt, J = 8.2, 4.1 Hz, 1H), 7.63 (dt, J = 6.9, 3.4 Hz, 1H), 3.60 (t, J = 7.2 Hz, 1H), 3.31 (t, J = 6.8 Hz, 1H), 1.82 (p, J = 6.8 Hz, 1H), 1.62 (q, J = 7.2 Hz, 1H), 1.45 – 1.35 (m, 1H). ^{13}C NMR (100 MHz, Chloroform-*d*) δ 168.21, 133.85, 132.03, 123.09, 37.56, 33.38, 32.13, 27.65, 25.33. MS (*m/z*): 296.2 (calc. 296.0 $[C_{13}H_{14}BrNO_2]H^+$).

*2.2.1.2. General procedure for the preparation of **10-13***

Compound **5** (5.67 g, 12 mmol) was added into MeCN (50 mL), and then Compound **6-9** (14.2 mmol) were added, respectively. After an addition of K_2CO_3 (5.9 g, 42.6 mmol), the mixture was refluxed for 24 h and followed by TLC. After the solvent was removed by distillation under reduced pressure, the residue was dissolved in EtOAc (200 mL), and washed by water (3×50 mL). The organic phase was dried by $MgSO_4$, and then was evaporated. The crude product was purified by column chromatography (DCM/EtOAc = 20:1, R_f = 0.7) to give **10-13** as white solid.

Compound **10** (2.0 g, yield 26%). ^{1}H NMR (400 MHz, Chloroform-*d*) δ 7.73 (dd, *J* = 5.4, 3.1 Hz, 2H), 7.61 (dd, *J* = 5.5, 3.1 Hz, 2H), 7.38 (d, *J* = 1.4 Hz, 1H), 6.09 (dd, *J* = 7.5, 5.9 Hz, 1H), 4.30 (dq, *J* = 6.1, 3.0 Hz, 1H), 4.27 – 4.16 (m, 2H), 3.95 (ddd, *J* = 6.4, 4.6, 2.0 Hz, 2H), 3.84 (q, *J* = 2.7 Hz, 1H), 3.74 (ddd, *J* = 41.4, 11.3, 2.7 Hz, 2H), 2.05 (ddd, *J* = 13.2, 5.9, 2.9 Hz, 1H), 1.88 (ddd, *J* = 13.4, 7.6, 6.1 Hz, 1H), 1.76 (d, *J* = 1.2 Hz, 3H), 0.88 (s, 9H), 0.82 (s, 9H), 0.06 (s, 6H), 0.01 (s, 3H), 0.00 (s, 3H). ^{13}C NMR (100 MHz, Chloroform-*d*) δ 168.31, 163.56, 150.96, 133.74, 133.65, 132.21, 123.10, 109.61, 87.83, 85.75, 72.02, 62.86, 41.45, 39.84, 36.12, 25.99, 25.78, 18.44, 18.01, 13.23, -4.58, -4.80, -5.32, -5.39. MS (*m/z*): 644.4 (calc. 644.3$[C_{32}H_{49}N_3O_7Si_2]H^+$).

Compound **11** (5.9 g, yield 68.2%). ^{1}H NMR (400 MHz, Chloroform-*d*) δ 7.82 (dd, *J* = 5.4, 3.0 Hz, 2H), 7.73 – 7.65 (m, 2H), 7.44 (d, *J* = 1.1 Hz, 1H), 6.32 (dd, *J* = 7.9, 5.8 Hz, 1H), 4.39 (dt, *J* = 5.6, 2.6 Hz, 1H), 4.04 (dd, *J* = 7.3, 2.6 Hz, 2H), 3.92 (q, *J* = 2.5 Hz, 1H), 3.89 – 3.70 (m, 4H), 2.25 (ddd, *J* = 13.1, 5.8, 2.6 Hz, 1H), 2.11 – 1.95 (m, 3H), 1.89 (d, *J* = 1.0 Hz, 3H), 0.92 (s, 9H), 0.89 (s, 9H), 0.11 (s, 6H), 0.08 (s, 3H), 0.07 (s, 3H). ^{13}C NMR (100 MHz, Chloroform-*d*) δ 168.42, 163.47, 150.91, 133.97, 133.64, 132.31, 123.35, 110.10, 87.89, 85.59, 72.38, 63.11, 41.56, 39.26, 36.08, 27.07, 26.09, 25.89, 18.54, 18.13, 13.40, -4.49, -4.69, -5.22, -5.30.

Compound **12** (4.7 g, yield 55%). ^{1}H NMR (400 MHz, Chloroform-*d*) δ 7.73 (tt, *J* = 5.0, 2.4 Hz, 2H), 7.62 (td, *J* = 5.2, 2.1 Hz, 2H), 7.36 (d, *J* = 1.1 Hz, 1H), 6.26 (dd, *J* = 7.9, 5.8 Hz, 1H), 4.33 (dt, *J* = 5.4, 2.5 Hz, 1H), 3.94 – 3.83 (m, 3H), 3.74 (ddd, *J* = 39.1, 11.4, 2.6 Hz, 2H), 3.63 (t, *J* = 6.5 Hz, 2H), 2.18 (ddd, *J* = 13.1, 5.8, 2.6 Hz, 1H), 1.98 – 1.89 (m, 1H), 1.82 (d, *J* = 1.0 Hz, 3H), 1.71 – 1.49 (m, 4H), 0.85 (s, 9H), 0.81 (s, 9H), 0.04 (s, 6H), 0.0025 (s, 3H), -0.0032 (s, 3H). ^{13}C NMR (100 MHz, Chloroform-*d*) δ 168.25, 163.32, 150.78, 133.79, 133.39, 132.15, 123.10, 109.91, 87.70, 85.41, 72.25, 62.96, 41.40, 40.73, 37.62, 26.17, 25.93, 25.74, 25.10, 18.37,

17.96, 13.24, -4.64, -4.84, -5.37, -5.46. MS (*m/z*): 672.6 (calc. 672.4 $[C_{34}H_{53}N_3O_7Si_2]H^+$).

Compound 13 (colorless oil, 7.1 g, yield 86%). ^{1}H NMR (400 MHz, Chloroform-d) δ 7.78 (tt, *J* = 5.0, 2.4 Hz, 2H), 7.72 – 7.61 (m, 2H), 7.39 (d, *J* = 1.1 Hz, 1H), 6.30 (dd, *J* = 7.8, 5.8 Hz, 1H), 4.36 (dt, *J* = 5.5, 2.5 Hz, 1H), 3.89 (tt, *J* = 7.7, 4.3 Hz, 3H), 3.77 (ddd, *J* = 39.5, 11.4, 2.6 Hz, 2H), 3.64 (t, *J* = 7.2 Hz, 2H), 2.22 (ddd, *J* = 13.1, 5.8, 2.6 Hz, 1H), 1.96 (ddd, *J* = 13.4, 8.0, 6.2 Hz, 1H), 1.86(d, *J* = 1.0 Hz, 3H), 1.64 (ddd, *J* = 18.8, 15.2, 7.5 Hz, 4H), 1.36 (d, *J* = 8.1 Hz, 2H), 1.30 – 1.15 (m, 2H), 0.89 (s, 9H), 0.85 (s, 9H), 0.07 (s, 6H), 0.04 (s, 3H), 0.03 (s, 3H). ^{13}C NMR (100 MHz, Chloroform-*d*) δ 168.41, 163.46, 150.91, 133.85, 133.40, 132.31, 123.21, 110.04, 87.80, 85.52, 72.34, 63.06, 41.51, 41.10, 37.89, 28.37, 27.26, 26.99, 26.02, 25.83, 24.34, 18.47, 18.06, 13.32, -4.55, -4.75, -5.29, -5.37. MS (*m/z*): 686.5 (calc. 686.4 $[C_{35}H_{55}N_3O_7Si_2]H^+$).

*2.2.1.3. General procedure for the preparation of **14-17***

Compound **10-13** (6.5 mmol) was dissolved in ethanol (50 mL), respectively. Then the hydranzine hydrate (80%) (2.0 mL) was added. The reaction mixture was stirred over night at room temperature. In the course of reaction, a white precipitate formed which was removed by filtration after the completion of the reaction. The solvent and excess $H_2N{\cdot}NH_2$ were evaporated under reduced pressure. The crude mixture was purified by column chromatography (DCM/MeOH = 10:1, R_f = 0.4) to give **14-17**.

Compound **14** (white soild, 2.1 g, yield 63%). ^{1}H NMR (400 MHz, Chloroform-*d*) δ 7.29 (s, 1H), 6.18 (t, *J* = 6.6 Hz, 1H), 4.24 (dt, *J* = 5.9, 2.7 Hz, 1H), 3.85 (t, *J* = 5.9 Hz, 2H), 3.76 (s, 1H), 3.72 – 3.55 (m, 2H), 2.77 (t, *J* = 6.1 Hz, 2H), 2.13 – 2.03 (m, 1H), 1.84 (dt, *J* = 13.1, 6.8 Hz, 1H), 1.75 (t, *J* = 2.1 Hz, 3H), 1.41 (s, 2H), 0.76 (s, 9H), 0.72 (s, 9H), -0.06 (s, 6H), -0.08 (s, 3H), -0.09 (s, 3H). ^{13}C NMR (100 MHz, Chloroform-*d*) δ 163.39, 150.83, 133.32, 109.66, 87.47, 85.22, 72.00, 62.73, 43.70, 41.16, 39.92, 25.73, 25.53, 18.15, 17.74, 13.06, -4.85, -5.05, -5.59, -5.66. MS (*m/z*): 514.4 (calc. 514.3 $[C_{24}H_{47}N_3O_5Si_2]H^+$).

Compound **15** (white soild, 2.3 g, yield 69.2%). ^{1}H NMR (400 MHz, Chloroform-*d*) δ 8.47 (s, 2H), 7.51 (s, 1H), 6.38 – 6.22 (m, 1H), 4.38 (dt, *J* = 5.7, 2.7 Hz, 1H), 4.10 (t, *J* = 6.2 Hz, 2H), 3.92 (q, *J* = 2.5 Hz, 1H), 3.80 (ddd, *J* = 44.7, 11.4, 2.5 Hz, 2H), 3.00 (t, *J* = 6.3 Hz, 2H), 2.25 (ddt, *J* = 20.7, 12.7, 6.1 Hz, 3H), 1.98 (dt, *J* = 13.5, 6.8 Hz, 1H), 1.90 (s, 3H), 0.91 (s, 9H), 0.88 (s, 9H), 0.09 (s, 6H), 0.07 (s, 3H), 0.06 (s, 3H). ^{13}C NMR (100 MHz, Chloroform-*d*) δ 164.41, 151.08, 134.51, 110.12, 88.03, 85.81,

72.27, 63.03, 41.70, 38.06, 37.04, 26.10, 25.91, 25.47, 18.56, 18.15, 13.38, -4.45, -4.69, -5.20, -5.27. MS (*m/z*): 528.3 (calc. 528.3 $[C_{25}H_{49}N_3O_5Si_2]H^+$).

Compound **16** (light yellow oil, 2.95 g, yield 84%). ^{1}H NMR (400 MHz, Chloroform-*d*) δ 7.43 – 7.34 (m, 1H), 6.29 (dd, *J* = 7.9, 5.8 Hz, 1H), 4.33 (dt, *J* = 5.4, 2.5 Hz, 1H), 3.94 – 3.82 (m, *J* = 7.3 Hz, 3H), 3.74 (ddd, *J* = 39.5, 11.4, 2.6 Hz, 2H), 2.65 (t, *J* = 7.0 Hz, 2H), 2.19 (ddd, *J* = 13.1, 5.8, 2.6 Hz, 1H), 1.98 – 1.88 (m, 1H), 1.88 – 1.80 (m, 3H), 1.59 (p, *J* = 7.5 Hz, 2H), 1.42 (p, *J* = 7.4 Hz, 4H), 0.85 (s, 9H), 0.82 (s, 9H), 0.04 (s, 6H), 0.01 (s, 3H), 0.00 (s, 3H). ^{13}C NMR (100 MHz, Chloroform-*d*) δ 163.45, 150.87, 133.38, 110.01, 87.76, 85.45, 72.30, 63.01, 41.80, 41.44, 41.05, 30.99, 25.96, 25.77, 24.90, 18.41, 18.00, 13.30, -4.61, -4.81, -5.34, -5.43. MS (*m/z*): 542.4 (calc. 542.3 $[C_{26}H_{51}N_3O_5Si_2]H^+$).

Compound **17** (white solid 1.8 g, yield 40%). ^{1}H NMR (400 MHz, Chloroform-*d*) δ 7.44 (d, *J* = 1.2 Hz, 1H), 6.36 (dd, *J* = 7.9, 5.8 Hz, 1H), 4.40 (dt, *J* = 5.5, 2.5 Hz, 1H), 4.00 – 3.89 (m, 3H), 3.81 (ddd, *J* = 40.3, 11.3, 2.6 Hz, 2H), 2.73 (t, *J* = 7.0 Hz, 2H), 2.26 (ddd, *J* = 13.1, 5.8, 2.6 Hz, 1H), 2.17 (s, 2H), 1.99 (ddd, *J* = 13.3, 7.9, 6.0 Hz, 1H), 1.92 (d, *J* = 1.1 Hz, 3H), 1.64 (p, *J* = 7.5 Hz, 2H), 1.53 (p, *J* = 7.3 Hz, 2H), 1.44 – 1.34 (m, 2H), 0.92 (s, 9H), 0.89 (s, 9H), 0.11 (s, 6H), 0.08 (s, 3H), 0.07 (s, 3H). ^{13}C NMR (100 MHz, Chloroform-*d*) δ 163.56, 150.57, 133.64, 109.74, 87.59, 85.34, 72.01, 62.78, 41.31, 40.87, 39.89, 26.75, 25.84, 25.64, 23.73, 18.28, 17.86, 13.25, -4.71, -4.95, -5.46, -5.54. HRMS (*m/z*): 556.3596 (calc. 556.3596 $[C_{27}H_{53}N_3O_5Si_2]H^+$).

*2.2.1.4. General procedure for the preparation of **18-21***

Compound **14-17** was dissolved into ethanol (70 mL), respectively. After an addition of concentrated hydrochloric acid (2.0 mL), the mixture was stirred for 12 h at room temperature and followed by TLC. After completing the reaction, the solvent was removed under reduced pressure and the crude product was purified by column chromatography (DCM/MeOH = 4:1, R_f = 0.4) to give **18-21**.

Compound **18** (white solid, yield 97%). ^{1}H NMR (400 MHz, Deuterium Oxide) δ 7.67 (s, 1H), 6.27 (t, *J* = 6.6 Hz, 1H), 4.45 (dt, *J* = 6.3, 4.1 Hz, 1H), 4.13 – 3.95 (m, 3H), 3.80 (ddd, *J* = 40.3, 11.3, 2.6 Hz, 2H), 2.92 (t, *J* = 6.4 Hz, 2H), 2.47 – 2.25 (m, 2H), 1.90 (s, 3H). ^{13}C NMR (100 MHz, Deuterium Oxide) δ 165.38, 151.67, 135.62, 110.44, 86.64, 85.88, 70.40, 61.17, 42.51, 38.83, 38.48, 12.38. MS (*m/z*): 286.2 (calc. 286.1 $[C_{12}H_{19}N_3O_5]H^+$).

Compound **19** (white solid, yield 92%). ^{1}H NMR (400 MHz, Deuterium Oxide) δ 7.64

(s, 1H), 6.25 (t, *J* = 6.7 Hz, 1H), 4.47 – 4.38 (m, 1H), 3.98 (t, *J* = 6.6 Hz, 3H), 3.77 (ddd, *J* = 40.3, 11.3, 2.6 Hz, 2H), 3.00 (t, *J* = 7.4 Hz, 2H), 2.41 – 2.25 (m, 2H), 1.98 (p, *J* = 6.9 Hz, 2H), 1.87 (s, 3H). ^{13}C NMR (100 MHz, Deuterium Oxide) δ 165.49, 151.64, 135.79, 110.57, 86.60, 85.93, 70.44, 61.24, 38.71, 38.39, 37.12, 25.09, 12.37. MS (*m/z*): 300.1 (calc. 300.2 $[C_{13}H_{21}N_3O_5]H^+$). HRMS (*m/z*): 322.1375 (calc. 322.1373 $[C_{13}H_{21}N_3O_5]Na^+$).

Compound **20** (white solid, 3.5 g, yield 97.8%). ^{1}H NMR (400 MHz, Methanol-d_4) δ 7.87 (d, *J* = 1.2 Hz, 1H), 6.31 (t, *J* = 7.2 Hz, 1H), 4.41 (dt, *J* = 6.4, 3.4 Hz, 1H), 3.97 (td, *J* = 6.7, 3.3 Hz, 2H), 3.93 (p, *J* = 3.4, 3.0 Hz, 1H), 3.77 (ddd, *J* = 40.3, 11.3, 2.6 Hz, 2H), 2.99 (t, J = 7.4 Hz 2H), 2.27 (ddd, *J* = 13.5, 6.2, 3.5 Hz, 1H), 2.22 (m, 1H), 1.91 (d, *J* = 1.2 Hz 3H), 1.69 (m, 4H). ^{13}C NMR (100 MHz, Deuterium Oxide) δ 164.99, 151.29, 135.49, 110.31, 86.62, 85.83, 70.46, 61.25, 40.71, 39.11, 38.85, 24.21, 23.90, 12.42. MS (*m/z*): 314.3 (calc. 314.2 $[C_{14}H_{23}N_3O_5]H^+$).

Compound **21** (white solid, yield 100%). ^{1}H NMR (400 MHz, Deuterium Oxide) δ 7.67 (s, 1H), 6.25 (t, *J* = 6.7 Hz, 1H), 4.46 (dt, *J* = 7.8, 4.0 Hz, 1H), 4.02 (d, *J* = 4.2 Hz, 1H), 3.91 – 3.72 (m, 4H), 3.03 (t, J = 7.6 Hz 2H), 2.44 – 2.26 (m, 2H), 1.89 (s, 3H), 1.72 (p, *J* = 7.6 Hz, 2H), 1.60 (p, *J* = 7.5 Hz, 2H), 1.40 (p, *J* = 7.6 Hz, 2H). ^{13}C NMR (100 MHz, Deuterium Oxide) δ 165.13, 151.40, 148.40, 135.49, 110.43, 86.64, 85.90, 70.52, 61.32, 41.24, 39.43, 38.94, 26.39, 23.10, 12.52. MS (*m/z*): 328.2 (calc. 328.2 $[C_{15}H_{25}N_3O_5]H^+$).

*2.2.1.5. General procedure for the preparation of thymidine dithiocarbamates**1-4***

Carbon disulfide (0.5 mL) was added into water (5 mL) containing aminothymidine with different carbon chain lengths (1.0 g), and then, 1.1 equivalents of NaOH or KOH was added. The reaction mixture was stirred for 3 h in an ice-water bath. The solvent removed under reduced pressure and the residue was recrystallized using isopropanol to give **1-4** as white solid.

Compound **1** (400 mg, 30%). ^{1}H NMR (400 MHz, Methanol-d_4) δ 7.83 (s, 1H), 6.28 (t, *J* = 6.5 Hz, 1H), 4.41 (dt, *J* = 5.9, 4.0 Hz, 1H), 4.23 – 4.13 (m, 2H), 3.93 – 3.89 (m, 1H), 3.86 – 3.70 (m, 4H), 3.35 (s, 1H), 2.36 – 2.15 (m, 2H), 1.92 (s, 3H). ^{13}C NMR (100 MHz, Methanol-d_4) δ 215.61, 165.68, 152.60, 136.57, 110.75, 88.73, 87.31, 71.83, 62.67, 47.14, 41.35, 40.98, 13.23. IR (KBr)/cm^{-1}: 3331.21, 2920.35, 1693.57, 1662.71, 1631.85, 1473.68, 1265.36, 1089.83, 1057.04. HRMS (*m/z*): 384.0662 (calc. 384.0658 $[C_{13}H_{18}N_3O_5S_2Na]H^+$).

Compound **2** (450 mg, 32.5%). ^{1}H NMR (400 MHz, Methanol-d_4) δ 7.84 (s, 1H), 6.31

(t, J = 6.6 Hz, 1H), 4.45 (dt, J = 7.3, 3.8 Hz, 1H), 4.00 (t, J = 6.6 Hz, 2H), 3.95 (q, J = 4.0, 3.5 Hz, 1H), 3.79 (ddd, J = 40.3, 11.3, 2.6 Hz, 2H), 3.55 (t, J = 6.7 Hz, 2H), 2.37 – 2.21 (m, 2H), 1.97 – 1.84 (m, 5H). ^{13}C NMR (100 MHz, Methanol-d_4) δ 214.43, 165.65, 152.57, 136.72, 110.87, 88.82, 87.25, 72.12, 62.90, 45.94, 41.24, 40.17, 28.03, 13.43. MS (*m/z*): 373.9 (calc. 374.1 $[C_{14}H_{20}N_3O_5S_2]^-$). IR (KBr)/cm^{-1}: 3321.56, 2926.14, 1693.57, 1664.64, 1631.85, 1473.68, 1280.79, 1093.69, 1055.11. HRMS (*m/z*): 374.0848 (calc. 374.0849 $[C_{14}H_{20}N_3O_5S_2]^-$).

Compound **3** (467mg, 34.2%). ^{1}H NMR (400 MHz, Methanol-d_4) δ 7.83 (s, 1H), 6.30 (t, J = 6.1 Hz, 1H), 4.40 (m, 1H), 4.05 – 3.88 (m, 4H), 3.86 – 3.70 (m, 2H), 3.58 (t, J = 6.4 Hz, 1H), 2.36 – 2.15 (m, 2H), 1.91 (s, 3H), 1.76 – 1.55 (m, 4H). ^{13}C NMR (100 MHz, Methanol-d_4) δ 214.17, 165.35, 152.27, 136.42, 110.66, 110.65, 88.78, 87.08, 72.03, 62.75, 42.00, 41.28, 27.16, 26.21, 13.25. IR (KBr)/cm^{-1}: 3346.64, 2922.28, 1691.64, 1664.64, 1629.92, 1469.82, 1280.79, 1076.33. HRMS (*m/z*): 388.1002 (calc. 388.1006 $[C_{15}H_{22}N_3O_5S_2]^-$)

Compound **4** (470mg, 36.0%). ^{1}H NMR (400 MHz, Methanol-d_4) δ 7.82 (s, 1H), 6.31 (t, J = 6.6 Hz, 1H), 4.43 (dt, J = 6.8, 3.7 Hz, 1H), 3.92 (m, 3H), 3.78 (m, 2H), 3.54 (t, J = 7.1 Hz, 2H), 2.36 – 2.18 (m, 2H), 1.91 (s, 3H), 1.70 – 1.56 (m, 4H), 1.43 – 1.29 (m, 2H). ^{13}C NMR (100 MHz, Methanol-d_4) δ 214.03, 165.31, 152.29, 136.37, 110.69, 88.74, 87.06, 72.02, 62.77, 48.61, 42.15, 41.18, 29.38, 28.35, 25.35, 13.25. IR (KBr)/cm^{-1}: 3319.63, 2933.85, 1693.57, 1664.64, 1631.85, 1471.75, 1269.22, 1097.54, 1057.04. HRMS (*m/z*): 402.1169 (calc. 402.1162 $[C_{16}H_{24}N_3O_5S_2]^-$).

2.2.2. Radiolabelling and quality control techniques

$^{99m}Tc(CO)_3$-DTC were prepared according to the previous reported methods [23, 35]. Namely, potassium sodium tartrate (15.0 mg), sodium carbonate (5.0 mg), sodium borohydride (10.0 mg) were added to a 10 mL glass vial. After sealing, the vial was flushed with CO for 15 min, followed by the addition of 1 mL of saline containing $^{99m}TcO_4^-$ (370 MBq). The mixture was heated at 80 ^{o}C for 30 min. After being cooled to the room temperature, the pH of fresh $[^{99m}Tc(CO)_3(H_2O)_3]^+$ was adjusted to approximately 7-8 using 1.0 mol/L HCl. Then, 1 mL of saline containing 1.0 mg of DTC and 0.5 mL of $[^{99m}Tc(CO)_3(H_2O)_3]^+$ precursor were added to a glass vial, and the mixture was incubated at room temperature for 20 min (Scheme 2). The radiochemical purities were determined by HPLC (High performance Liquid Chromatography). The elution conditions of HPLC were as follows. Water (containing 0.1 % TFA) (A) and acetonitrile (containing 0.1% TFA) (B) were used as

mobile phase. The gradient elution technique was adopted: 0 min 10% B, 2 min 10% B, 10 min 90% B, 18 min 90% B, 25 min 10% B.

2.2.3. Preparation of $Re(CO)_3$ complexes

To confirm the speculative structure of $^{99m}Tc(CO)_3$-labelled thymidine analogs, their corresponding rhenium-tricarbonyl complexes were also synthesized. Bromopentacarbonylrhenium (I) ([$Re(CO)_5$] Br) (20 mg) and water (about 5 mL) were added to a 10 mL pear-shaped flask, and then the mixture was heated to reflux for 24 h [36, 37]. Successively, 250 μL of the above solution (about 1.0 mg intermediate) was transferred into another 5 mL pear-shaped flask and 250 μL of dithiocarbamate derivatives (20.0 mg/mL) was added, and then was heated at 90 ^{o}C for 3 h (Scheme 2). After the completion of the reaction, the mixture solvent was purified by HPLC to obtain the $Re(CO)_3$ complexes.

1b: ^{1}H NMR (400 MHz, Methanol-d_4) δ 7.82 (s, 1H), 6.46 – 6.07 (m, 1H), 4.48 – 4.25 (m, 3H), 4.11 – 3.87 (m, 3H), 3.86 – 3.63 (m, 2H), 3.48 (s, 1H), 2.30 – 2.28 (m, 2H), 1.93 (s, 3H). IR (KBr)/cm^{-1}: 3414.15, 2015.70, 1907.68, 1701.29, 1635.71, 1099.47, 1058.97, 769.63. HRMS (*m/z*): 632.0167 (calc. 632.0171 [$C_{16}H_{20}N_3O_9S_2Re$-H_2O]H^+).

2b: ^{1}H NMR (400 MHz, Methanol-d_4) δ 7.87 (s, 1H), 6.31 (t, *J* = 6.6 Hz, 1H), 4.40 (dt, *J* = 6.4, 3.4 Hz, 1H), 4.10 – 3.94 (m, 2H), 3.92 (q, *J* = 3.2 Hz, 1H), 3.84 – 3.69 (m, 2H), 3.48 (dq, *J* = 11.9, 7.0, 5.7 Hz, 2H), 2.35 – 2.16 (m, 2H), 2.03 – 1.80 (m, 5H). IR (KBr)/cm^{-1}: 2015.70, 1901.89, 1689.72, 1621.13, 1473.68, 1082.11. HRMS (*m/z*): 646.0317 (calc. 646.0319 [$C_{17}H_{22}N_3O_9S_2Re$-H_2O]H^+).

3b: ^{1}H NMR (400 MHz, Methanol-d_4) δ 7.85 (s, 1H), 6.31 (t, *J* = 6.6 Hz, 1H), 4.40 (dt, *J* = 6.6, 3.4 Hz, 1H), 4.07 – 3.85 (m, 3H), 3.84 – 3.69 (m, 2H), 3.65 – 3.38 (m, 2H), 2.35 – 2.12 (m, 2H), 1.91 (s, 3H), 1.84 – 1.56 (m, 4H). IR (KBr)/cm^{-1}: 3396.79, 2930.00, 2013.77, 1901.89, 1695.50, 1664.64, 1627.99, 1467.89,1093.69, 1047.39. HRMS (*m/z*): 660.0473 (calc. 660.0476 [$C_{18}H_{24}N_3O_9S_2Re$-H_2O]H^+).

4b: ^{1}H NMR (400 MHz, Methanol-d_4) δ 7.85 (s, 1H), 6.31 (t, *J* = 6.6 Hz, 1H), 4.40 (dt, *J* = 6.7, 3.5 Hz, 1H), 4.02 – 3.86 (m, 2H), 3.77 (ddd, *J* = 30.1, 12.0, 3.4 Hz, 2H), 3.52 – 3.39 (m, 1H), 2.34 – 2.13 (m, 2H), 2.09 – 1.98 (m, 1H), 1.91 (s, 3H), 1.67 (dp, *J* = 16.2, 8.1, 7.7 Hz, 3H), 1.49 – 1.21 (m, 6H). IR (KBr)/cm^{-1}: 2920.35, 2011.84, 1896.11, 1629.92, 1103.33, 1058.97. HRMS (*m/z*): 674.0638 (calc. 674.0632 [$C_{19}H_{26}N_3O_9S_2Re$-H_2O]H^+);

2.2.4. In vitro stability study

The complexes were incubated in the labelling saline at room temperature for 6 h, and then the stability of complex was determined by HPLC. On the other hand, 0.1 mL (3.7-7.4 MBq) of **1a**, **2a**, **3a**, and **4a** were added to 0.1 mL of mouse serum and incubated at 37 ^{o}C for 6 h, respectively. After removal of the proteins using acetonitrile, the RCP (Radiochemical purities) of the complexes were measured by HPLC.

2.2.5. Determination of the partition coefficient

In order to evaluate the complex's lipophilicity, the partition coefficient of the complex between phosphate buffer (0.025 mol/L, pH = 7.4) and 1-octanol was measured. In a 2 mL centrifuge tube, 0.1 mL of the labeled complex solution was added, followed by an addtion of 0.9 mL of phosphate buffer (0.025 mol/L, pH = 7.4) and 1.0 mL of 1-octanol. The centrifuge tube was shacked on a Vortex mixer for 30 seconds and then centrifuged at 5000 rpm for another 5 min. Three samples (100 μL) from each layer in triplets were measured by gamma counter. The partition coefficient was calculated as follow: P = (counters per minute in 1-octanol/counters per minute in phosphate buffer). Usually, log P was the final expression of the partition coefficient. Samples from the 1-octanol layer were redistributed until consistent distribution coefficient values were obtained.

2.2.6. In vitro cell uptake experiments

HCT116 cell line was obtained from China Infrastructure of Cell Line Resource and was maintained as manufacturer's recommendations. Cells suspended in 1 mL of culture medium were seeded into 24-well plates (0.1×10^{6} cells/well). The plates were incubated for 48 h in a 5% CO_2-humidified atmosphere at 37 ^{o}C. The medium was removed and washed with 0.5 mL fresh culture medium. 0.1 mL medium containing 74 kBq technetium-99m complex and 0.4 mL fresh medium or 0.4 mL fresh medium containing 2.0 mg thymidine were added into the well. After incubated for 2 h at 37 ^{o}C or 4 °C, the medium was removed and the cells were washed with 2 × 0.5 mL cold PBS (4 ^{o}C, 0.01 M, pH = 7.4). After detached by addition of 0.5 mL 1M NaOH , the cells were collected and counted in a gamma counter (Wizard 2480, PerkinElmer). The protein content was measured spectrophotometrically using a Micro BCA protein assay reagent (Macgene, Beijing, China).The results were expressed as a ratio of the percentage of the initial activity to the protein mass (% ID/mg protein). Each

experiment was performed three times. In the FU pretreatment assay, twenty-four hours after being seeded, the exponentially cells were exposed to 100 μM 5-FU for another 24 h.

2.2.7. Biodistribution study

All the biodistribution studies were carried out in compliance with the national laws related to the ethics during experimentation. Approximate 2×10^6 S180 cells were implanted in the left front left armpit of male mice by subcutaneous injection. After one week, tumors grew to diameters of 7-10 mm. 0.1 mL of $^{99m}Tc(CO)_3$-labelled radiotracer (37 kBq) was injected into the mice bearing S180 tumor via a tail vein. The mice were sacrificed by neck dislocation at 0.5 h, 2 h, and 4 h post-injection. The tumors, interesting organs and blood were collected, weighed and measured for radioactive counts. The results were expressed as the percent uptake of injected dose per gram of tissue (% ID/g).

2.2.8. SPECT imaging study

A Triumph SPECT/CT scanner (TriFoil Imaging, California, USA), a dual-modality scanner supporting CT and SPECT imaging acquisition, was used for SPECT/CT imaging studies. 0.1 mL of **1a** (11.1 MBq) was injected intravenously through tail vein into a Kunming mouse bearing S180 tumor. After anesthetized with 1.5% isoflurane in air, the mouse was fixed near the center of the SPECT/CT scanner. Static imaging was obtained at 120 min after injection.

3. Results and discussion

3.1. Synthesis and radiolabelling

Compound **1-4**, dithiocarbamate derivatives of TdR functionalized at position N3, were synthesized via five steps from thymidine, and the reaction equations were shown in Scheme 1. Intermediates and the final ligands were identified by ^{1}H-NMR, ^{13}C-NMR, MS or HRMS, and the results showed that the target ligands were successfully synthesized.

The H_2O in the *fac*-$[^{99m}Tc(CO)_3(H_2O)_3]^+$ precursor was easily substituted by sulfur atoms in the dithiocarbamate [32, 38], and then $^{99m}Tc(CO)_3$-dithiocarbamates (**1a-4a**) were prepared (Scheme 2). In order to study the structure of **1a-4a**, the corresponding rhenium complexes (**1b-4b**) were synthesized according to the previous literature

[36]. When ^{99m}Tc and Re complexes were co-injected in HPLC, the retention time of radioactivity and UV detectors provided strong evidence for confirmation (Figure 1).

Radiochemical purities (RCP) of the complexes were measured by HPLC. The retention times of the precursor *fac*-[^{99m}Tc(CO)$_3$(H$_2$O)$_3$]$^+$ and ^{99m}TcO$_4^-$ were 12.17 min and 3.93 min, respectively. While the retention times of **1a**-**4a** were 13.52 min, 13.85 min, 13.93 min and 14.18 min, respectively. The results of HPLC analysis showed that the RCP of the radiotracers were more than 90%.

3.2. In vitro stability study and partition coefficients

The complexes were stable over 4 h under different conditions, including in the reaction mixture at room temperature, and also in the mouse serum at 37 ^{o}C, suggesting that they had a high stability *in vitro*.

The log *P* values of **1a-4a** were 0.65 ± 0.07, 0.82 ± 0.06, 0.93 ± 0.05 and 1.08 ± 0.07, respectively. The results suggested that they were lipophilic. Moreover, the log *P* values of the corresponding ^{99m}Tc(CO)$_3$ complexes are in accordance with the structure of the ligands, since incorporation of more CH$_2$ group increases the lipophilicity.

3.3. Cell uptake experiments

The thymidine kinase 1 is located in the cytosol, and the potential imaging complex has to pass through the cell membrane before it can be phosphorylated. If this transport is not achieved actively via nucleoside transporters, then it must occur by passive diffusion [39]. In order to investigate the major cell internalization routes of the complex **1a-4a**, the incorporations of these complexes were evaluated in HCT116 colorectal carcinoma cells. The HCT116 cell line was chosen for its TK1 overexpression and prominent selectivity of the enzyme for thymidine and thymidine analogs [40, 41]. Internalization was measured with and without pretreatment with 5-FU (5-fluorouracil) [20, 41], and with excessive thymidine. 5-FU, a thymidylate synthase inhibitor, is known to increase the uptake of 5-iododeoxyuridine or ^{18}F-FLT, via inhibiting endogenous thymidine synthesis, increasing the levels of TK1 and inducing re-distribution of nucleoside transporters [41-44]. The results of internalization experiments were presented in Figure 2.

In the previous literatures, researchers proposed that uptakes of N3 functionalized thymidine complexes occurred via passive diffusion and endocytosis [20, 45, 46]. In

the present work, pretreatment with 5-FU and blocking with thymidine, had an effect on the uptake of **1a-4a** on tumor cells. For **1a** and **2a**, lower temperature could significantly reduce the tumor uptake of the radioactivity, but as the carbon chain lengthened, the effect of temperature on cell uptake disappeared. The above experiment showed that the uptakes of $^{99m}Tc(CO)_3$-labelled thymiding dithiocarbamate derivatives were mediated, at least in part, by nucleoside transporters, especially the uptakes of **1a** and **2a**.

3.4. Biodistribution study

The results of biodistributions of **1a-4a** in mice bearing S180 tuomor were shown in Table 1 and Table 2. These four radiotracers had similar biological properties. The tumor uptakes of those complexes were quite high and the retentions of them were perfect. Taking **1a** as an example, the tumor uptake of **1a** was 3.28 ± 1.10% ID/g at 30 min post-injection, and the tumor uptake was still 2.95 ± 0.73% ID/g at 240 min post-injection, suggesting that the complex had a good retention in tumor. At the same time, the complex had a good tumor/muscle ratio. In other rapidly growing organs, such as the spleen and intestine, the uptakes were 2.2-fold and 7.7-fold higher than that of muscle at 120 min post-injection. Interestingly, the uptake of the complex in the liver gradually increased with time, and the trend of kidney uptake was consistent. Like many radionuclide labelled thymidine or tymidine derivatives [47-50], activity accumulation in the kidney and liver showed that the major route of excretion was renal and hepatobiliary. The tumor uptake values of complex 4a were significantly lower than those of the other three complexes, indicating that the elongation of the carbon chain didn't cause an increase in the tumor uptake. Low uptake in the thyroid suggested that there was no $^{99m}TcO_4^-$ derived from the decompostion of the complex *in vivo*.

Table 1. Biodistrbutions of **1a** and **2a** in mice bearing S180 tumor (mean ± SD, n = 5, % ID/g).

	1a ($^{99m}Tc(CO)_3$-DTC-2-TdR)			**2a** ($^{99m}Tc(CO)_3$-DTC-3-TdR)		
% ID/g	30 min	120 min	240 min	30 min	120 min	240 min
Heart	3.08±0.45	2.02±0.18	1.59±0.27	4.04±0.75	2.83±0.30	1.63±0.32
Liver	15.28±2.59	19.48±3.94	24.91±2.90	33.79±3.36	46.71±3.42	46.40±5.03
Lung	6.74±1.57	3.45±0.69	3.70±0.85	11.70±3.52	6.34±0.77	4.99±0.89
Kidney	14.89±2.70	16.43±2.24	18.55±2.77	15.21±2.35	18.27±2.29	15.77±1.96
Spleen	1.75±0.31	1.38±0.30	1.11±0.16	5.26±1.87	3.24±1.78	2.76±1.65

Stomach	1.77±0.78	1.98±0.70	2.40±0.59	0.63±0.22	0.64±0.31	0.60±0.14
Bone	1.58±0.25	1.16±0.12	1.01±0.15	2.67±0.40	1.73±0.30	0.98±0.20
Muscle	0.87±0.22	0.63±0.34	0.66±0.12	0.91±0.18	0.78±0.12	0.61±0.21
Intestine	8.42±2.74	4.88±2.60	4.04±0.82	6.08±1.00	3.82±0.52	2.67±0.40
Tumor	3.28±1.10	3.35±0.51	2.95±0.73	3.98±0.91	3.99±0.58	4.29±0.88
Blood	13.33±1.56	7.75±0.51	5.54±0.27	20.62±3.18	9.93±1.66	5.67±1.65
Thyroid [a]	0.06±0.03	0.06±0.02	0.05±0.01	0.05±0.03	0.04±0.02	0.02±0.01
T/B	0.25	0.43	0.53	0.19	0.40	0.76
T/M	3.77	5.29	4.50	4.35	5.09	7.03

[a] Expressed as % injected dose per organ (% ID)
T/B = tumor-to-blood ratio, T/M = tumor-to-muscle ratio

Table 2. Biodistrbutions of **3a** and **4a** in mice bearing S180 tumor (mean ± SD, n = 5, % ID/g).

	3a (^{99m}Tc(CO)$_3$-DTC-4-TdR)			**4a** (^{99m}Tc(CO)$_3$-DTC-5-TdR)		
% ID/g	30 min	120 min	240 min	30 min	120 min	240 min
Heart	4.43±0.56	2.80±0.40	2.06±0.30	1.61±0.24	1.29±0.17	1.11±0.19
Liver	25.28±1.57	32.76±3.47	36.34±2.82	37.93±3.93	40.76±5.77	38.64±7.04
Lung	9.48±1.81	6.00±0.78	4.60±0.36	4.00±0.72	2.97±0.35	2.63±0.59
Kidney	14.77±1.36	15.21±0.63	15.42±1.89	10.79±1.60	12.59±0.93	11.47±1.28
Spleen	5.70±2.88	3.41±1.93	2.29±0.41	1.57±0.25	1.22±0.22	1.11±0.26
Stomach	0.95±0.11	1.00±0.25	1.05±0.28	0.77±0.37	1.11±0.42	1.06±0.22
Bone	2.57±0.33	1.72±0.17	1.18±0.15	1.35±0.45	0.99±0.21	0.97±0.18
Muscle	1.01±0.10	0.99±0.25	0.67±0.10	0.46±0.12	0.52±0.14	0.43±0.08
Intestine	4.49±1.03	3.32±0.38	2.72±0.17	3.87±0.98	2.86±0.94	2.38±1.36
Tumor	3.75±1.36	3.80±0.91	3.60±0.27	1.84±0.54	1.87±0.52	1.88±0.36
Blood	18.21±2.15	9.22±2.05	5.92±0.65	6.04±0.93	3.68±0.15	2.99±0.95
Thyroid [a]	0.09±0.05	0.07±0.02	0.05±0.01	0.03±0.02	0.03±0.01	0.02±0.01
T/B	0.21	0.41	0.60	0.31	0.51	0.63
T/M	3.73	3.85	5.41	3.97	3.57	4.36

[a] Expressed as % injected dose per organ (% ID)
T/B = tumor-to-blood ratio, T/M = tumor-to-muscle ratio

Table 3. showed some results of biodistribution of previously reported radionuclide labelled thymidine derivatives. When compared to the complexes ^{99m}Tc(CO)3-12N3-5-TdR (functionalized at N3 position) [23] and ^{99m}Tc-TMHEA (functionalized at C5 position) [22], **1a** exhibited a much higher tumor uptake. The tumor uptake of **1a** (3.35±0.51% ID/g) was more than five times higher than that of

^{99m}Tc(CO)$_3$-12N3-5-TdR (0.63±0.14% ID/g), and more than six times higher than that of ^{99m}Tc-TMHEA (0.51±0.05% ID/g) at 2 h post-injection. As for the tumor-to-muscle ratio, **1a** was also higher than the other two complexes.

Table 3. Comparison of biodistribution of some reported ^{99m}Tc labelled thymidine derivatives.

complex	**1a**	^{99m}Tc(CO)$_3$-12N3-5-TdR	^{99m}Tc-TMHEA
Time p.i (h)	2	2	2
Tumor uptake (% ID/g)	3.35±0.51	0.63±0.14	0.51±0.05
Tumor/Muscle	5.29	2.88	2.84
Labelling core	^{99m}Tc(CO)$_3$	^{99m}Tc(CO)$_3$	^{99m}TcO
Tumor models	S180	S180	HepA
Reference	Present study	23	22

3.5. SPECT imaging studies

Because **1a** (^{99m}Tc(CO)$_3$-DTC-2-TdR) showed a high tumor uptake and a lower liver uptake, it was selected as a promising candidate for imaging studies. The solid tumor could be clearly visualized with high tumor-to-background contrast (Figure 3), suggesting **1a** exhibited its potential as a tumor imaging agent. However, the liver uptake of **1a** was appreciable, thus making it unsuitable to localize tumor in liver. The imaging findings were similar to the biodistribution results in mice. Low uptake in the thyroid suggested good in vivo stability of **1a**.

4. Conclusion

In the present study, we synthesized four novel thymidine derivatives, functionalized at position N3. Their corresponding ^{99m}Tc(CO)$_3$-labelled complexes were successfully prepared in high yields via a ligand-exchange reaction. The complexes were lipophilic and stable *in vitro*. Cell uptake studies showed that they were transported via

nucleoside transporters. The biodistributions and SPECT imaging studies in mice bearing S180 tumor showed that they had an obvious tumor uptake and high tumor/muscle ratio. In this case, **1a** revealed promising biological features as a potential tracer for tumor proliferation imaging, justifying further investigations.

Acknowledgements

The work was financially supported, in part, by the National Natural Science Foundation of China (21771023), the foundation of Key Laboratory of Radiopharmaceuticals (Beijing Normal University), Ministry of Education.

Conflicts of interest

There are no conflicts to declare

Notes and references

[1] K. Herholz, J. Rudolf, W.D. Heiss, FDG transport and phosphorylation in human gliomas measured with dynamic PET, J.Neuro-Oncol. 12 (1992) 159-165.

[2] M.G. Vander Heiden, L.C. Cantley, C.B. Thompson, Understanding the Warburg effect: the metabolic requirements of cell proliferation, Sci. 324 (2009) 1029-1033.

[3] R. Kubota, S. Yamada, K. Kubota, K. Ishiwata, N. Tamahashi, T. Ido, Intratumoral distribution of fluorine-18-fluorodeoxyglucose *in vivo*: high accumulation in macrophages and granulation tissues studied by microautoradiography, J. Nucl. Med. 33 (1992) 1972-1980.

[4] D. Hanahan, R.A. Weinberg, Hallmarks of cancer: the next generation, Cell 144 (2011) 646-674.

[5] J. Shelton, X. Lu, J.A. Hollenbaugh, J.H. Cho, F. Amblard, R.F. Schinazi, Metabolism, biochemical actions, and chemical synthesis of anticancer nucleosides, nucleotides, and base analogs, Chem. Rev. 116 (2016) 14379-14455.

[6] P. Perlíková, M. Hocek, Pyrrolo[2,3-*d*]pyrimidine (7-deazapurine) as a privileged scaffold in design of antitumor and antiviral nucleosides, Med. Res. Rev. 37 (2017) 1429-1460.

[7] K. Kowalski, Ferrocenyl-nucleobase complexes: Synthesis, chemistry and applications, Coord. Chem. Rev. 317 (2016) 132-156.

[8] Skiba Joanna, Yuan Qing, Hildebrandt Alexander, Lang Heinrich, Trzybiński Damian, Woźniak Krzysztof, Balogh Ria Katalin, Gyurcsik Béla, Vrček

Valerije, Kowalski Konrad: Ferrocenyl GNA nucleosides: a bridge between organic and organometallic xeno-nucleic acids, ChemPlusChem. 83(2018)77-86.

[9] M.D. Bartholomae, A.R. Vortherms, S. Hillier, B. Ploier, J. Joyal, J. Babich, R.P. Doyle, J. Zubieta, Synthesis, cytotoxicity, and insight into the mode of action of $Re(CO)_3$ thymidine complexes, ChemMedChem. 5 (2010) 1513-1529.

[10] A.F. Shields, J.R. Grierson, B.M. Dohmen, H.-J. Machulla, J.C. Stayanoff, J.M. Lawhorn-Crews, J.E. Obradovich, O. Muzik, T.J. Mangner, Imaging proliferation in vivo with [F-18] FLT and positron emission tomography, Nat. Med. 4 (1998) 1334-1336.

[11] J.R. Bading, A.F. Shields, Imaging of cell proliferation: status and prospects, J. Nucl. Med. 49 Suppl 2 (2008) 64S-80S.

[12] M. Peck, H.A. Pollack, A. Friesen, M. Muzi, S.C. Shoner, E.G. Shankland, J.R. Fink, J.O. Armstrong, J.M. Link, K.A. Krohn, Applications of PET imaging with the proliferation marker ^{18}F -FLT, Q. J. Nucl. Med. Mol. Imaging 59 (2015) 95-104.

[13] R. Schibli, M. Netter, L. Scapozza, M. Birringer, P. Schelling, C. Dumas, J. Schoch, P.A. Schubiger, First organometallic inhibitors for human thymidine kinase: synthesis and in vitro evaluation of rhenium(I)- and technetium(I)-tricarbonyl complexes of thymidine, J. Organomet. Chem. 668 (2003) 67-74.

[14] M. Schmid, B. Neumaier, A.T. Vogg, K. Wczasek, C. Friesen, F.M. Mottaghy, A.K. Buck, S.N. Reske, Synthesis and evaluation of a radiometal-labeled macrocyclic chelator-derivatised thymidine analog, Nucl. Med. Biol. 33 (2006) 359-366.

[15] S. Celen, T. de Groot, J. Balzarini, K. Vunckx, C. Terwinghe, P. Vermaelen, L. Van Berckelaer, H. Vanbilloen, J. Nuyts, L. Mortelmans, A. Verbruggen, G. Bormans, Synthesis and evaluation of a ^{99m}Tc-MAMA-propyl-thymidine complex as a potential probe for in vivo visualization of tumor cell proliferation with SPECT, Nucl. Med. Biol. 34 (2007) 283-91.

[16] M. Stichelberger, D. Desbouis, V. Spiwok, L. Scapozza, P.A. Schubiger, R. Schibli, Synthesis, in vitro and in silico assessment of organometallic rhenium(I) and technetium(I) thymidine complexes, J. Organomet. Chem. 692 (2007) 1255-1264.

[17] B. Teng, Y.P. Bai, Y. Chang, S.Z. Chen, Z.L. Li, Technetium-99m-labeling and synthesis of thymidine analogs: potential candidates for tumor imaging, Bioorg. Med. Chem. Lett. 17 (2007) 3440-3444.

[18] D. Desbouis, H. Struthers, V. Spiwok, T. Kuster, R. Schibli, Synthesis, in vitro, and in silico evaluation of organometallic technetium and rhenium thymidine

complexes with retained substrate activity toward human thymidine kinase type 1, J. Med. Chem. 51 (2008) 6689-6698.

[19] H. Struthers, B. Spingler, T.L. Mindt, R. Schibli, "Click-to-Chelate": Design and incorporation of triazole-containing metal-chelating systems into biomolecules of diagnostic and therapeutic interest, Chem. Eur. J. 14 (2008) 6173-6183.

[20] H. Struthers, D. Viertl, M. Kosinski, B. Spingler, F. Buchegger, R. Schibli, Charge dependent substrate activity of C3' and N3 functionalized, organometallic technetium and rhenium-labeled thymidine derivatives toward human thymidine kinase 1, Bioconj. Chem. 21 (2010) 622-634.

[21] L. Chun Xiong, W. Zheng Wu, J. Quan Fu, T. Jie, T. Cheng, Z. Jian Kang, Synthesis and preliminary biological evaluation of a technetium-99m labeled thymidine analog, Chin. Chem. Lett. 22 (2011) 1309-1312.

[22] C. Lu, Q. Jiang, C. Tan, J. Tang, J. Zhang, Preparation and preliminary biological evaluation of novel ^{99m}Tc-labelled thymidine analogs as tumor imaging agents, Molecules 17 (2012) 8518-8532.

[23] X. Duan, T. Liu, Y. Zhang, J. Zhang, Synthesis and biological evaluation of novel $^{99m}Tc(CO)_3$-labeled thymidine analogs as potential probes for tumor proliferation imaging, Molecules 21 (2016) 510-522.

[24] J.B. Zhang, X.B. Wang, C.Y. Li, Synthesis and biodistribution of a new ^{99m}Tc nitrido complex for cerebral imaging, Nucl. Med. Biol. 29 (2002) 665-669.

[25] J. Zhang, H. Guo, S. Zhang, Y. Lin, X. Wang, Synthesis and biodistribution of a novel ^{99m}TcN complex of ciprofloxacin dithiocarbamate as a potential agent for infection imaging, Bioorg. Med. Chem. Lett. 18 (2008) 5168-5170.

[26] J. Zhang, Y. Lin, X. Sheng, X. Wang, Synthesis of a novel ^{99m}Tc nitrido radiopharmaceutical with isopropyl xanthate, showing brain uptake, Appl. Radiat. Isot. 67((2009) 79-82.

[27] J. Zhang, J. Ren, X. Lin, X. Wang, Synthesis and biological evaluation of a novel ^{99m}Tc nitrido radiopharmaceutical with deoxyglucose dithiocarbamate, showing tumor uptake, Bioorg. Med. Chem. Lett. 19 (2009) 2752-2754.

[28] J. Zhang, Z. Song, X. Wang, Synthesis of a bis(2,3-dimethylcyclohexyl-dithiocarbamato)-nitrido ^{99m}Tc complex: A potential tracer for myocardial imaging, Appl. Radiat. Isot. 67 (2009) 577-580.

[29] J. Zhang, S. Zhang, H. Guo, X. Wang, Synthesis and biological evaluation of a novel $^{99m}Tc(CO)_3$ complex of ciprofloxacin dithiocarbamate as a potential agent to target infection, Bioorg. Med. Chem. Lett. 20 (2010) 3781-3784.

[30] S. Zhang, W. Zhang, Y. Wang, Z. Jin, X. Wang, J. Zhang, Y. Zhang, Synthesis and biodistribution of a novel ^{99m}TcN complex of norfloxacin fithiocarbamate as a potential agent for bacterial infection imaging, Bioconj. Chem. 22 (2011) 369-375.

[31] X. Lin, Z. Jin, J. Ren, Y. Pang, W. Zhang, J. Huo, X. Wang, J. Zhang, Y. Zhang, Synthesis and biodistribution of a new ^{99m}Tc-oxo complex with deoxyglucose dithiocarbamate for tumor imaging, Chem. Biol. Drug Des. 79 (2012) 239-245.

[32] Z. Li, X. Song, J. Zhang, Synthesis and biological evaluation of novel ^{99m}Tc labeled ornidazole xanthate complexes as potential hypoxia imaging agents, J. Radioanal. Nucl. Chem. 306 (2015) 535-542.

[33] J.M.J. Tronchet, I. Kovacs, P. Dilda, M. Seman, G. Andrei, R. Snoeck, E. De Clereq, J. Balzarini, Synthesis and anti-HIV activity of thymidine analogues bearing a 4 '-cyanovinyl group and some derivatives thereof, Nucleos. Nucleot. Nucl. 20 (2001) 1927-1939.

[34] L. Cheng, Z. Jiang, J. Dong, B. Cai, Y. Yang, X. Li, C. Chen, Monolayers of novel gemini amphiphiles with phthalimide headgroups at the air/water interface: pH and alkyl chain length effects, J. Colloid Interface Sci. 401 (2013) 97-106.

[35] R. Alberto, R. Schibli, A.P. Schubiger, U. Abram, H.J. Pietzsch, B. Johannsen, First application of fac-$[Tc\text{-}99m(OH_2)_3(CO)_3]^+$ in bioorganometallic chemistry: Design, structure, and in vitro affinity of a 5-HT_{1A} receptor ligand labeled with ^{99m}Tc, J. Am. Chem. Soc. 121 (1999) 6076-6077.

[36] Q. Xue, H. Wang, J. Liu, D. Wang, H. Zhang, Synthesis and biodistribution of novel dipicolylamine ^{99m}Tc-$(CO)_3$-labeled fatty acid derivatives for myocardial imaging, J. Radioanal. Nucl. Chem. 310 (2016) 1181-1194.

[37] N. Lazarova, S. James, J. Babich, J. Zubieta, A convenient synthesis, chemical characterization and reactivity of $[Re(CO)_3(H_2O)_3]Br$: the crystal and molecular structure of $[Re(CO)_3(CH_3CN)_2Br]$, Inorg. Chem. Commun. 7 (2004) 1023-1026.

[38] X. Lin, X. Chao, J. Zhang, Z. Jin, Y. Zhang, Preparation and biodistribution of a ^{99m}Tc tricarbonyl complex with deoxyglucose dithiocarbamate as a tumor imaging agent for SPECT, Bioorg. Med. Chem. Lett. 24 (2014) 3964-3967.

[39] J. Zhang, F. Visser, K.M. King, S.A. Baldwin, J.D. Young, C.E. Cass, The role of nucleoside transporters in cancer chemotherapy with nucleoside drugs, Cancer Metastasis Rev. 26 (2007) 85-110.

[40] E.T. McKinley, G.D. Ayers, R.A. Smith, S.A. Saleh, P. Zhao, M.K. Washington, R.J. Coffey, H.C. Manning, Limits of F-18 -FLT PET as a biomarker of proliferation in oncology, PLOS One 8 (2013) e58938.

[41] S.J. Lee, S.Y. Kim, H.C. Jin, S.J. Oh, S.R. Jin, S.H. Yong, T.W. Kim, D.H. Moon, Induction of thymidine kinase 1 after 5-fluorouracil as a mechanism for 3'-deoxy-3'-[^{18}F]fluorothymidine flare, Biochem. Pharmacol. 80 (2010) 1528-1536.

[42] Y.M. Dupertuis, M. Vazquez, J.P. Mach, N. De Tribolet, C. Pichard, D.O. Slosman, F. Buchegger, Fluorodeoxyuridine improves imaging of human glioblastoma xenografts with radiolabeled iododeoxyuridine, Cancer Res. 61 (2001) 7971-7977.

[43] M. Perumal, R.G. Pillai, H. Barthel, J. Leyton, J.R. Latigo, M. Forster, F. Mitchell, A.L. Jackman, E.O. Aboagye, Redistribution of nucleoside transporters to the cell membrane provides a novel approach for imaging thymidylate synthase inhibition by positron emission tomography, Cancer Res. 66 (2006) 8558-8564.

[44] J. Pressacco, B. Mitrovski, C. Erlichman, D.W. Hedley, Effects of thymidylate synthase inhibition on thymidine kinase activity and nucleoside transporter expression, Cancer Res. 55 (1995) 1505-1508.

[45] M.D. Bartholoma, A.R. Vortherms, S. Hillier, J. Joyal, J. Babich, R.P. Doyle, J. Zubieta, Synthesis, cytotoxicity and cellular uptake studies of N3 functionalized $Re(CO)_3$ thymidine complexes, Dalton Trans. 40 (2011) 6216-6225.

[46] Y. Byun, J.H. Yan, A.S. Al-Madhoun, J. Johnsamuel, W.L. Yang, R.F. Barth, S. Eriksson, W. Tjarks, Synthesis and biological evaluation of neutral and zwitterionic 3-carboranyl thymidine analogues for boron neutron capture therapy, J. Med. Chem. 48 (2005) 1188-1198.

[47] G. Sokal, In vivo measurement of carbon-11 thymidine uptake in non-Hodgkin's lymphoma using positron emission tomography, J. Nucl. Med. 29 (1988) 1633-1637.

[48] A.F. Shields, S.M. Larson, Z. Grunbaum, M.M. Graham, Short-term thymidine uptake in normal and neoplastic tissues: studies for PET, J. Nucl. Med. 25 (1984) 759-764.

[49] U. Mukhopadhyay, S. Soghomonyan, H.H. Yeh, L.G. Flores, A. Shavrin, A.Y. Volgin, J.G. Gelovani, M.M. Alauddin, N^3-Substituted thymidine analogues V:

Synthesis and preliminary PET imaging of N^3-[^{18}F]fluoroethyl thymidine and N^3-[^{18}F]fluoropropyl thymidine, Nucl. Med. Biol. 35 (2008) 697-705.

[50] R. Nishii, A.Y. Volgin, O. Mawlawi, U. Mukhopadhyay, A. Pal, W. Bornmann, J.G. Gelovani, M.M. Alauddin, Evaluation of 2'-deoxy-2'-[^{18}F]fluoro-5-methyl-1-β-$_L$-arabinofuranosyluracil ([^{18}F]-$_L$-FMAU) as a PET imaging agent for cellular proliferation: comparison with [^{18}F]-$_D$-FMAU and [^{18}F]FLT, Eur. J. Nucl. Med. Mol. Imaging 35 (2008) 990-998.

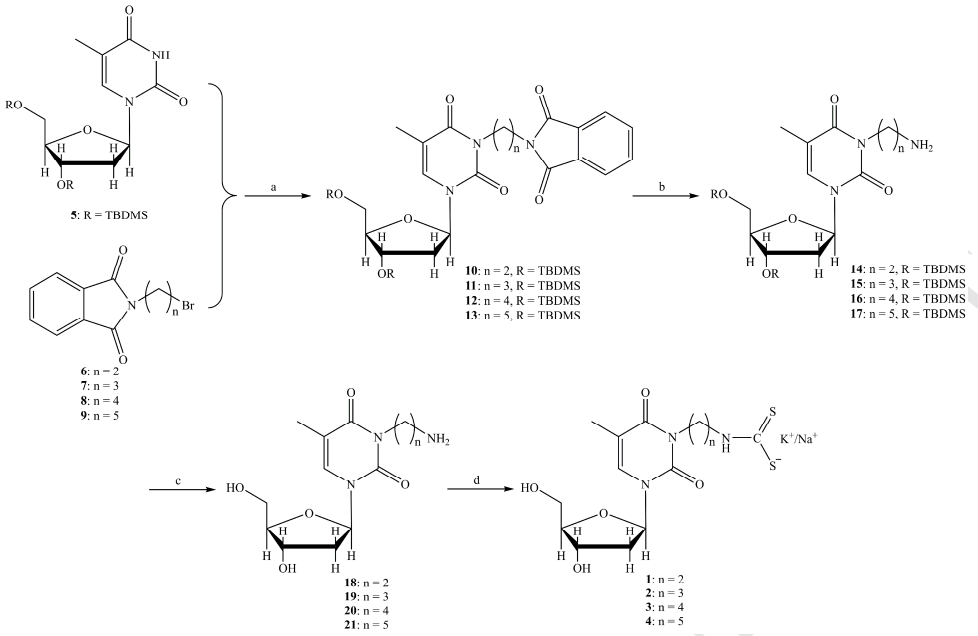

Scheme 1. The synthesis of thymidine dithiocarbamates. Reagents and conditions: (a) dibromoalkanes, MeCN, K_2CO_3, reflux, 24 h; (b) EtOH, hydranzine hydrate, r.t., 12 h; (c) EtOH, conc.HCl, 12 h; (d) CS_2, H_2O, NaOH/KOH, 0 ^oC, 3 h.

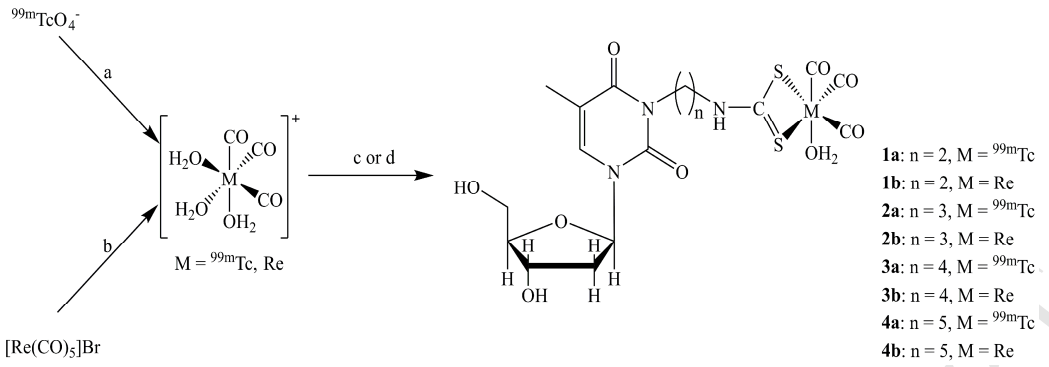

Scheme 2. Preparations procedures and speculative structures of $M(CO)_3$-labelled dithiocarbamate derivatives (M=^{99m}Tc, Re). Reagents and conditions: (a) M = ^{99m}Tc, $NaCO_3$, $NaBH_4$, potassium sodium tartrate, CO, 30 min, 80 ^{o}C; (b) M = Re, H_2O, 100 ^{o}C, 24 h; (c) M = ^{99m}Tc, DTC, pH = 7-8, 10-20 min, r.t.; (d) M = Re, DTC-TdR, H_2O, 90 ^{o}C, 3 h.

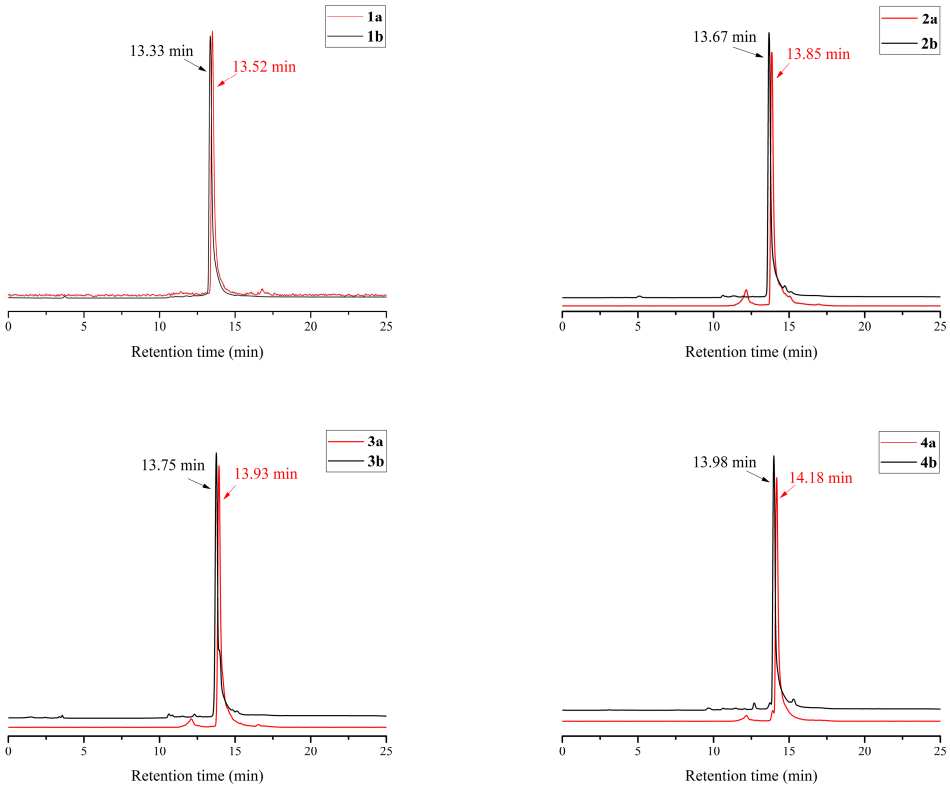

Figure 1. HPLC profiles of the $^{99m}Tc(CO)_3$-labelled radiotracers (red) and the corresponding $Re(CO)_3$ complexes (black).

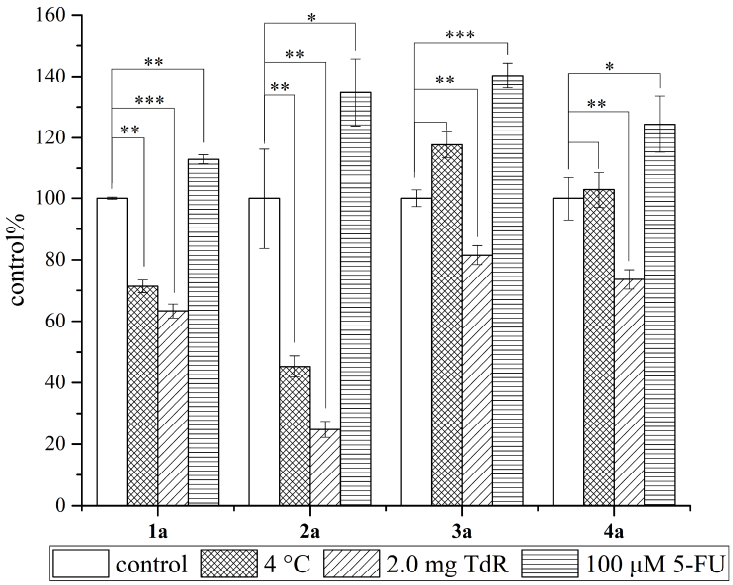

Figure 2. Cell uptakes on the human colorectal carcinoma HCT116 cell line over a period of 2 h at 37 ^{o}C, with and without pretreatment with 5-FU, and blocking experiments with 2.0 mg thymidine, and at 4 °C. Statistical significance was determined using a bilateral t test of equal variance. Statistical significance is reported for $^{*}p < 0.05$, $^{**}p < 0.01$ and $^{***}p < 0.001$.

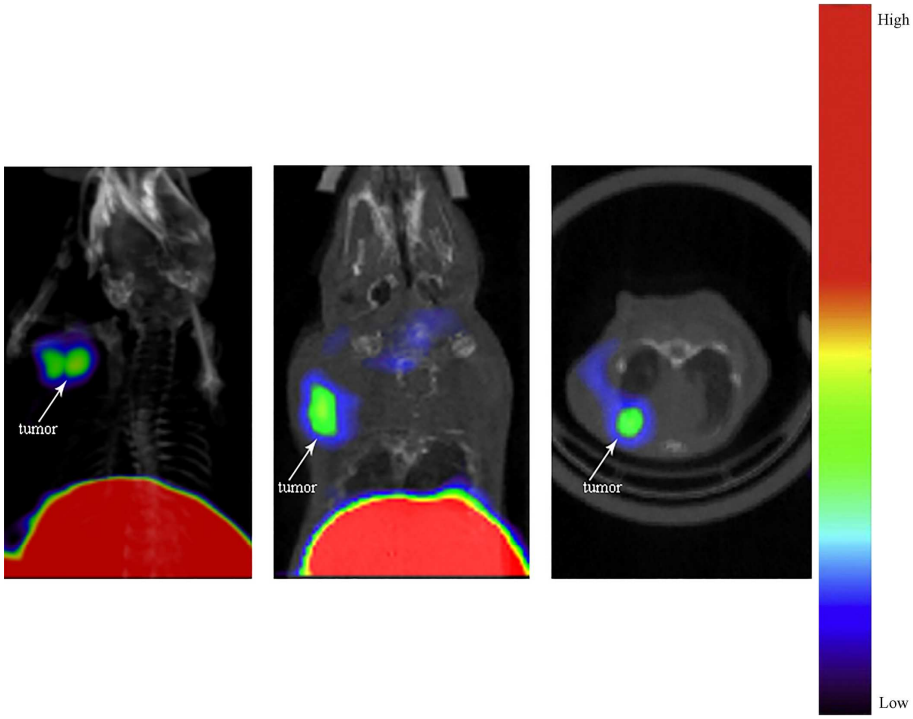

Figure 3. SPECT/CT image of 1a in S180 tumor-bearing mouse at 2 h post injection (left: visual image; middle: sagittal image; right: transversal image).

Highlights

- A series of novel $M(CO)_3$-labelled thymidine dithiocarbamate derivatives were prepared (M = ^{99m}Tc, Re).
- Some of the complexes entered the cell via the transport of the nucleoside transporters.
- $^{99m}Tc(CO)_3$-labelled complexes had high tumor uptake and good tumor/muscle ratio and the SPECT imaging studies in mice bearing tumor showed that one of the complexes had an obvious tumor uptake and high tumor-to-background ratio.